

Optimal Deep Learning-Based Recognition Model for EEG Enabled Brain-Computer Interfaces Using Motor-Imagery

S. Rajalakshmi^{1*}, Ibrahim AlMohimeed², Mohamed Yacin Sikkandar², S. Sabarunisha Begum³

¹*Department of Artificial Intelligence and Data Science, Dr. N. G. P. Institute Technology, Coimbatore, India, mrajislm@hotmail.com*

²*Department of Medical Equipment Technology, College of Applied Medical Science, Majmaah University, Majmaah, Saudi Arabia, i.almohimeed.@mu.edu.sa, m.sikkandar@mu.edu.sa*

³*Department of Biotechnology, PSR Engineering College, Sivakasi, India, sabarunishabegum@psr.edu.in*

Abstract: Brain-Computer Interfaces (BCIs) facilitate the translation of brain activity into actionable commands and act as a crucial link between the human brain and the external environment. Electroencephalography (EEG)-based BCIs, which focus on motor imagery, have emerged as an important area of study in this domain. They are used in neurorehabilitation, neuroprosthetics, and gaming, among other applications. Optimal Deep Learning-Based Recognition for EEG Signal Motor Imagery (ODLR-EEGSM) is a novel approach presented in this article that aims to improve the recognition of motor imagery from EEG signals. The proposed method includes several crucial stages to improve the precision and effectiveness of EEG-based motor imagery recognition. The pre-processing phase starts with the Variation Mode Decomposition (VMD) technique, which is used to improve EEG signals. The EEG signals are decomposed into different oscillatory modes by VMD, laying the groundwork for subsequent feature extraction. Feature extraction is a crucial component of the ODLR-EEGSM method. In this study, we use Stacked Sparse Auto Encoder (SSAE) models to identify significant patterns in the pre-processed EEG data. Our approach is based on the classification model using Deep Wavelet Neural Network (DWNN) optimized with Chaotic Dragonfly Algorithm (CDFA). CDFA optimizes the weight and bias values of the DWNN, significantly improving the classification accuracy of motor imagery. To evaluate the efficacy of the ODLR-EEGSM method, we use benchmark datasets to perform rigorous performance validation. The results show that our approach outperforms current methods in the classification of EEG motor imagery, confirming its promising performance. This study has the potential to make brain-computer interface applications in various fields more accurate and efficient, and pave the way for brain-controlled interactions with external systems and devices.

Keywords: Deep Learning (DL), Brain-Computer Interface (BCI), EEG Motor Imagery (MI), classification, Dragonfly algorithm, feature extraction.

1. INTRODUCTION

Brain-Computer Interface (BCI) is a transmission control scheme determined between the brain and external devices (computer or other electronic devices) via a signal generated during brain activity [1]. The scheme does not depend on nerves and muscles, except the brain, and establishes a direct transmission between the machine and the brain. It is an advanced and higher-end human-computer communication technique. The Motor Imagery Brain-Computer Interface (MI BCI) based Electroencephalogram (EEG) belongs to the class of brain-computer interaction [2]. Nowadays, there are two brain-computer interaction techniques: invasive and non-invasive. Non-invasive BCI is commonly employed due to its low cost and convenient operation [3]. Using the non-invasive BCI, we can obtain various patterns of brain activity signals, which are widely investigated and used in pattern recognition, signal processing, medicine, rehabilitation,

cognitive science, etc. [4]. The study of EEG signal scan occasionally helps individuals who can no longer function independently due to injuries to the nerves or muscles that control limb movement, such as strokes, craniocerebral nerve injuries, spinal injuries, etc. [5]. The patient is unable to control their body independently, and in severe cases, they cannot even interact with the patient.

EEG signals are used to study the patient's brain activity. This helps the patient to interact with the outside world, improves the quality of day to day lives, and reduces the mental burden [6]. Motor imagery could induce sensorimotor concussion, activate the sensorimotor cortex, reflect the subject's motor intention, and emit EEG signals [7]. Once the subject visualizes some portion of the limb movement instead of the real movement, the corresponding reflex area in the human brain would show electrical potential change. By examining the changes in the electrical potential of the EEG

signal and detecting the motion pattern visualized by the present subject, an external device is controlled to assist the subject in performing the respective movement task. Therefore, the study of EEG signals and the detection of movement intentions is very important in the fields of medical treatment with artificial intelligence [8]-[11].

2. RELATED WORKS

Huang et al. [12] presented a Deep Learning (DL) technique based on EEG signal to improve MI classification efficiency by introducing the Local Reparameterization Trick into Convolution Neural Network (LRT-CNN). 109 subjects from the PhysioNet Data set were used to test the presented approach. First, a global classification was estimated by four groups. Next, individual variability was investigated by testing with individual subjects. The researchers in [13] developed a feature extraction approach that results in a potential MI classification efficiency. The connection matrix indicates the correlation between distinct channel temporal blocks. They form the dynamic connectivity pattern, which consists of three-dimensional tensors. Then, the kernel Principal Component Analysis (PCA) or a nonlinear convolution autoencoder is applied to this tensor to learn a discriminative representation. Musallam et al. [14] designed TCNet-Fusion, a fixed hyperparameter based CNN method that uses different approaches, namely the layer fusion, Temporal Convolution Network (TCN), distinguishable convolution, and depth-wise convolution. The method outperformed other fixed hyperparameter-based CNN approaches when left analogous to a variable hyperparameter network.

Zhang et al. [15] developed a CNN framework for robust and accurate EEG-based MI classification. The presented approach, which includes EEG-inception, is based on the mainstream of the inception-time network, which has been shown to be extremely accurate and effective for time-sequence classification. Moreover, the presented method is an end-to-end classification since it uses the raw EEG signal as input and does not require complicated EEG signal-preprocessing. The researchers in [16] used different data preprocessing methods and investigated their influence on the classification efficiency of a Feed Forward Neural Network (FFNN). Since the results with the FFNN were not acceptable, the data developed with the optimal preprocessing approach were used for CNN training. The Harmony search approach is used for feature selection. Finally, the Long Short Term Memory - Deep Neural Network (LSTM-DNN) method is used to classify EEG data. The alpha and beta waves are taken into account. For feature extraction and pre-processing of EEG data, the LSTM-DNN method is used to prove its effectiveness.

3. PROPOSED MODEL

In this article, a new Optimal Deep Learning-Based Recognition for EEG Signal Motor Imagery (ODLR-EEGSM) technique approach for the classification of EEG motor imagery for BCI systems was developed. The presented ODLR-EEGSM technique approach includes VMD-based pre-processing, Stacked Sparse Auto Encoder (SSAE)-based feature extraction, Deep Wavelet Neural

Network (DWNN)-based classifier, and CDFA-based parameter optimization. The application of the Chaotic Dragonfly Algorithm (CDFA) for parameter tuning of the DWNN model (i.e., tuning the weight and bias values of the DWNN model) helps to improve the classification results. Fig. 1 shows the general block diagram of the ODLR-EEGSM technique.

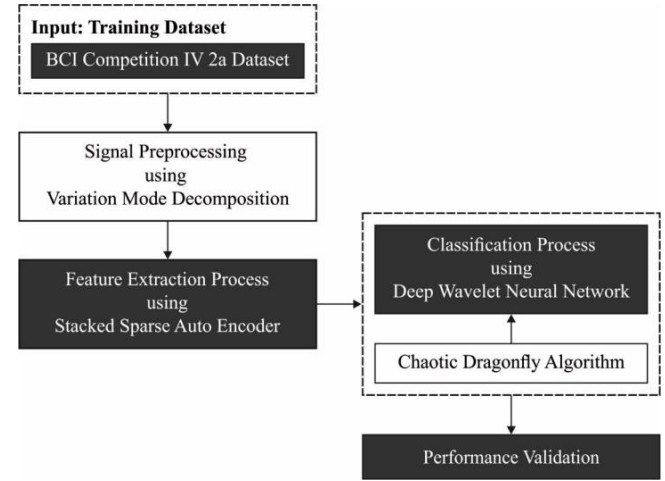


Fig. 1. General block diagram of ODLR-EEGSM technique.

A. Pre-processing using the VMD approach

Variation Mode Decomposition (VMD) includes a non-recursive technique for simultaneous mode extraction in a signal. This technique forms a group of techniques in which the input signal is recreated using the least squares principle. This technique is also very robust to noise. Wiener Filtering (WF) and Hilbert transform were used in the VMD approach. This approach addresses the occurrence of noise in the input signals. It is distributed by using WF. Using the Hilbert transform rule, a unilateral spectrum was created from the VMD approach. The center frequency is unique for the sub-bands calculated using this approach. When the modes in the input signals were removed, the center frequency of the modes was removed by multiplying by an exponential value tuned to the respective center frequency. The resulting constrained variational issue is formulated as:

$$\min\{u_k\}, \{\omega_k\} \left\{ \sum_k^n \left\| \delta_t \left[\left(\delta(t) + \frac{j}{\pi t} \right) * u_k(t) \right] e^{-j\omega t} \right\|_2^2 \right\} \quad (1)$$

subjected to $\sum_k^n u_k = f$, where f refers to the input signals. $\{u_k\} = \{u_1, u_2, \dots, u_K\}$ indicates the group of modes and $\{\omega_k = \omega_1, \omega_2, \dots, \omega_K\}$ demonstrates the group of all center frequencies.

All modes are changed to process analytical signals using the Hilbert transform, which is used to extract the unilateral frequency spectrum. All modes are multiplied by an exponential value tuned to the value of the center frequencies. The bandwidth constraints are calculated by performing the squared L^2 norm of the achieved gradients. The center frequency was calculated for the sub-bands of a11300 EEG signal and the result was examined.

B. SSAE based feature extraction

During the feature extraction process, the pre-processed EEG motor imagery is fed into the SSAE model to derive feature vectors. Auto Encoder (AE) is frequently used for non-linear dimensionality reduction, in particular AE [19] consists of an encoder layer and a decoder layer, which is FFNN. Similar to PCA, AE is mostly used for dimensionality reduction of data. In the encoder layer, AE receives $x \in R^p$ as input and encodes x in the hidden layer h to reduce the input dimension; in the decoder layer, the decreased dimension data is decoded as output. An input vector was encoded as the formula:

$$h = \sigma(Wx + b) \quad (2)$$

where σ denoted the activation function, e.g., sigmoid, tanh, $W \in R^{n \times p}$ denotes the weighted matrix and $b \in R^n$ denotes the bias vector. Then, the hidden expression was decoded to obtain the data close to an input x utilizing by using the decoder formula:

$$\hat{x} = \sigma(W'h + b') \quad (3)$$

where $W' \in R^{p \times n}$ refers to the weighted matrix and $b' \in R^p$ denotes the bias vectors. The disparity between the input x and the resulting \hat{x} is called the reconstruction error. To optimize the parameters W, W', b, b' , the reconstruction error is used as a cost function. For a single trained instance, the cost function was demonstrated as the formula:

$$J_{AE} = \frac{1}{2} \|\hat{x} - x\|^2 \quad (4)$$

To obtain multiple trained instances, the entire cost function was demonstrated as the formula:

$$J_{AE} = \frac{1}{N} \sum_{i=1}^N \|\hat{x}^{(i)} - X(i)\|^2 \quad (5)$$

The over-fitting issue is a challenge for training the network of AE. Finally, the weighted penalty cost functions were executed, which are an effective method to solve over-fitting. The penalty cost function was determined as:

$$J_{AE} = \frac{1}{N} \sum_{i=1}^N \frac{1}{2} \|\hat{x}^{(i)} - x^{(i)}\|^2 + \frac{\lambda}{2} (\|W\|^2 + \|W'\|^2) \quad (6)$$

When the input dimensions are usually very large or the number of hidden units is enormous, sparsity was run against the hidden unit under the trained one to discover the particular input infrastructure. The neuron is assumed active if its resulting value is closer to 1, but inactive if its resulting value is closer to 0. The average activation of the hidden units j can be determined as:

$$\hat{\rho}_j = \frac{1}{N} \sum_{i=1}^N h_j(x^{(i)}) \quad (7)$$

To enforce sparsity, it can be limited $\hat{\rho}_j = \rho$, where ρ refers to the sparsity target and often has a smaller positive number near 0. Thus, an attempt is made to minimize the Kullback-Leibler (KL) divergence between $\hat{\rho}_j$ and ρ as follows:

$$J_{KL}(\rho \|\hat{\rho}_j) = \sum_{j=1}^S \rho \log \frac{\rho}{\hat{\rho}_j} + (1 - \rho) \log \frac{1 - \rho}{1 - \hat{\rho}_j} \quad (8)$$

where S is the number of hidden layer nodes. Thus, the entire cost function of sparse AE is:

$$J_{SAE} = \frac{1}{N} \sum_{i=1}^N \frac{1}{2} \|\hat{x}^{(i)} - x^{(i)}\|^2 + \frac{\lambda}{2} (\|W\|^2 + \|W'\|^2) + \beta J_{KL}(\rho \|\hat{\rho}_j) \quad (9)$$

where β denotes the sparsity penalty. With minimized cost functions, an optimal parameter W' , band b' is achieved. AE is more stacked to learn more informative features. The SSAE has been presented by using several AEs. As shown in the encoded layer, an input layer was connected to the following SAE to extract an optimal feature and so on.

C. Optimal DWNN based classification

In feature extraction, the pre-processed EEG motor imagery is fed into the SSAE model to derive feature vectors.

The DWNN model is used in the extraction process. It is a 4-layer model that includes an input layer, a Wavelon layer, a product layer, and an output layer. First, pre-processing is performed in the input layer, while the Wavelon layer processes the data using the wavelet activation function [20]. Deep feature extraction is performed by the translated and dilated version of the wavelet function. The product is validated in the product layer and the decision is offered in the output layer. The n dimension biased network with m nodes produces the result as given below:

$$\zeta = \omega^T \varphi(x, \tau, \sigma) + \mu^T \phi(x, \tau, \sigma) \quad (10)$$

where $x = [x_1, x_2, \dots, x_n]^T \in R^n$ denotes the input vector, $\tau = [\tau_1, \tau_2, \dots, \tau_m]^T \in R^{m \times n}$ and $\sigma = [\sigma_1, \sigma_2, \dots, \sigma_m]^T \in R^{m \times n}$ implies translation and dilation variables, $\phi = [\phi_1, \phi_2, \dots, \phi_m]^T \in \mathfrak{R}^m$ denotes a wavelet function and $[\phi_1, \phi_2, \dots, \phi_m]^T \in \mathfrak{R}^m$ denotes the corresponding bias function. The weights and the bias function can be denoted as: $\omega = [\omega_1, \dots, \omega_m]^T \in R^m$ and $\mu = [\mu_1, \dots, \mu_m]^T \in R^m$, respectively. The estimation function can be mathematically formatted as follows:

$$\hat{\zeta}(x(n)) = \hat{\omega}^T \hat{\phi}(x(n)) + \hat{\mu}^T \varphi(x(n)) \quad (11)$$

where $\hat{\omega}, \hat{\mu}$ denote the estimate of the optimal value of the network variable, ω^*, μ^* correspondingly. The optimization problem is formulated in terms of the estimation error, as given below:

$$\tilde{\zeta}(x(n)) = \zeta(x(n)) - \hat{\zeta}(x(n)) = \tilde{\omega}(n) \hat{\phi}(x(n)) + \tilde{\mu}(n) \varphi(x(n)) + \varepsilon(x(n)) \quad (12)$$

4. RESULT ANALYSIS

Performance validation of the Search and Rescue with a Continuous Butterfly Optimization Algorithm for Multihop Secure Routing (IV) model is tested using the EEG data of motor imagery from the BCI competition IV 2a dataset. It

contains data from 9 distinct subjects performing four processes, namely:

- left hand (class 1),
- right hand (class 2),
- feet (class 3), and
- tongue (class 4).

Fig. 2 shows a comprehensive accuracy examination of the SRCBO-MHSR model on different runs (Run) and subjects (Sub). The table values show that the SRCBO-MHSR model resulted in higher accuracy values for all Runs and Subs. For example, for Sub-1, the SRCBO-MHSR model achieved 92.56%, 93.86%, 93.84%, 94.25%, and 94.91% accuracy in Runs 1-5. For Sub-3, the SRCBO-MHSR model achieved 92.58%, 92.76%, 93.62%, 94.23%, and 94.56% accuracy in Runs 1-5, respectively. For Sub-4, the SRCBO-MHSR model achieved 92.56%, 92.60%, 92.60%, 92.61%, and 93.70% accuracy in Runs 1-5, respectively.

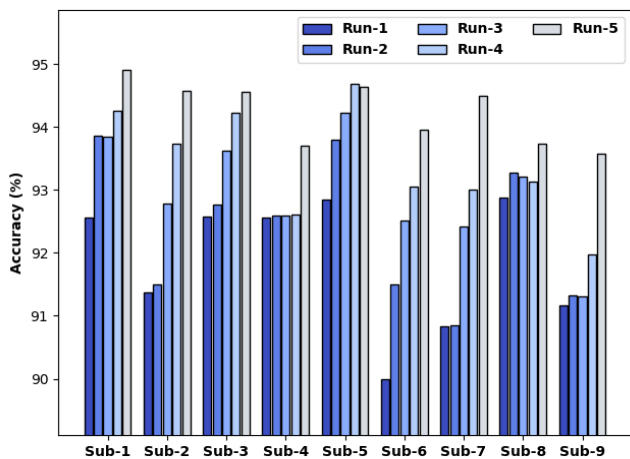


Fig. 2. Result analysis of the SRCBO-MHSR technique in terms of accuracy.

Fig. 3 shows the average accuracy analysis of the SRCBO-MHSR model in the classification of EEG motor imagery. From the figure, it can be seen that the SRCBO-MHSR model achieved a maximum average accuracy of 93.88% in Sub-1, 92.79% in Sub-2, 93.55% in Sub-3, 92.81% in Sub-4, 94.04% in Sub-5, 92.20% in Sub-6, and 91.87% in Sub-9.

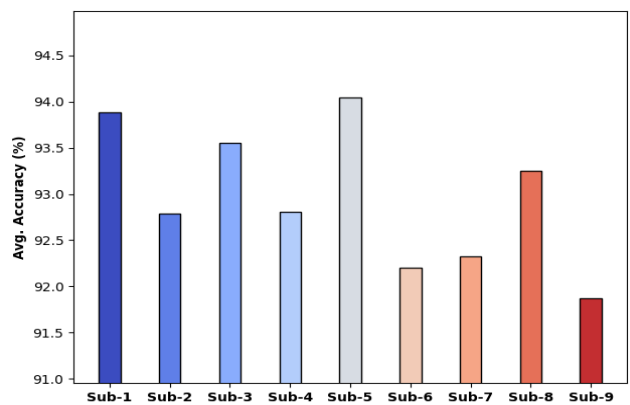


Fig. 3. Average accuracy analysis of the SRCBO-MHSR technique.

Fig.4 shows kappa investigation of the SRCBO-MHSR method under various Runs and Subs. For example, for Sub-1, the SRCBO-MHSR model achieved a kappa value of 91.47%, 91.55%, 91.84%, 92.14%, and 94.33% for Runs 1-5, respectively. Similarly, for Sub-3, the SRCBO-MHSR technique achieved a kappa of 91.36%, 91.85%, 92.95%, 93.64%, and 94.11% for Runs 1-5. Finally, for Sub-4, the SRCBO-MHSR method achieved a kappa of 92.61%, 92.92%, 94.44%, 94.44%, and 93.82% for Runs 1-5, respectively.

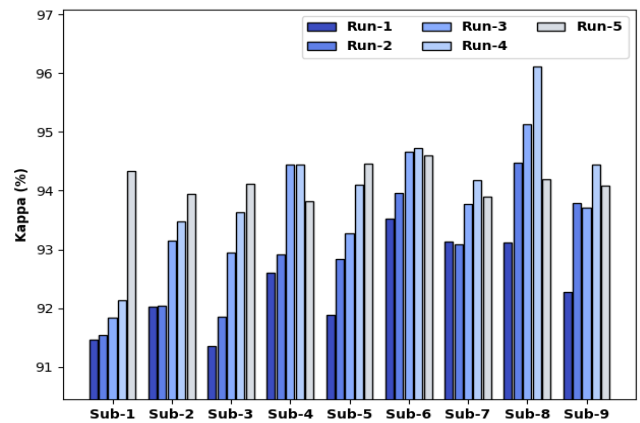


Fig. 4. Result analysis of the SRCBO-MHSR technique in terms of kappa.

Fig. 5 illustrates the average kappa analysis of the SRCBO-MHSR technique in the classification of EEG motor imagery. It can be seen from the figure that the SRCBO-MHSR approach resulted in a maximum average kappa of 93.88% for Sub-1, 92.27% for Sub-2, 92.93% for Sub-3, 92.78% for Sub-4, 93.65% for Sub-5, 93.31% for Sub-6, and 94.29% for Sub-9.

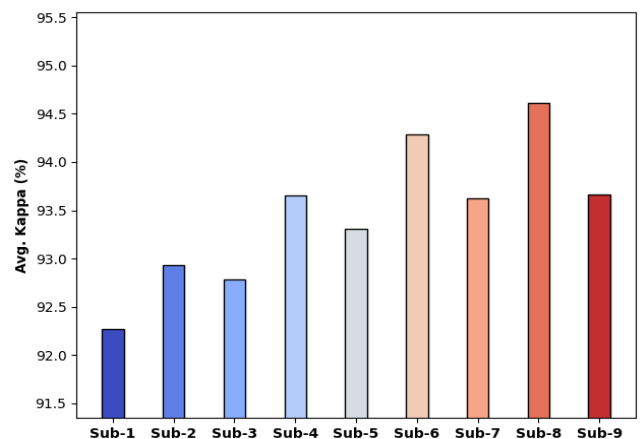


Fig. 5. Average kappa analysis of the SRCBO-MHSR technique.

The accuracy outcome analysis of the SRCBO-MHSR approach using the test data is shown in Fig. 6. The results show that the SRCBO-MHSR technique has achieved improved validation accuracy compared to the training accuracy. It is also observed that the accuracy values get saturated with the number of epochs.

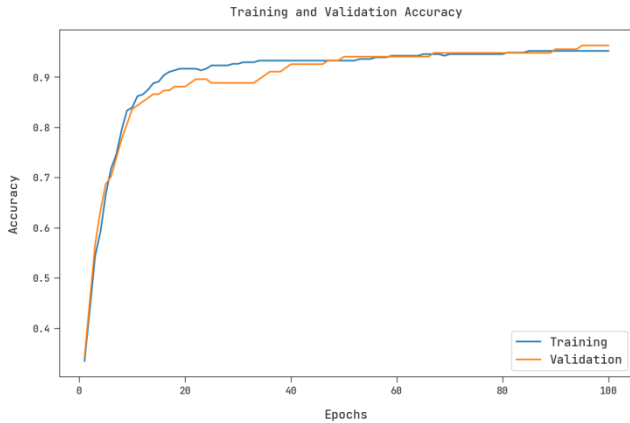


Fig. 6. Accuracy analysis of the SRCBO-MHSR technique.

The loss outcome analysis of the SRCBO-MHSR system on the test data is shown in Fig. 7. The figure shows that the SRCBO-MHSR technique has reduced the validation loss compared to the training loss. It can also be seen that the loss values get saturated with the number of epochs.

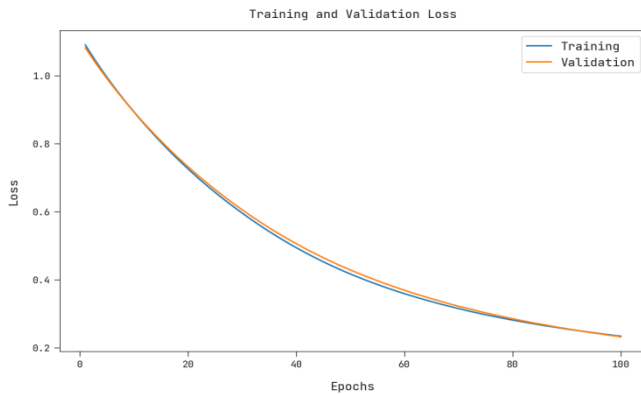


Fig. 7. Loss analysis of the SRCBO-MHSR technique.

Experimental results demonstrated that the SRCBO-MHSR model performed better than the other methods with maximum accuracy values in all subjects. For example, for Sub-1, the SRCBO-MHSR model achieved a higher accuracy of 93.88%, while the Channel Wise - Convolutional Neural Network (CW-CNN), Separable Common Spatial-Spectral Patterns (SCSSP), Densely Feature Fusion Convolutional Neural Network (DFFN), and Electroencephalography – Deep Machine Vision (EEG-DMV) models achieved a lower accuracy of 87.15%, 68.90%, 85.19%, and 87.70%, respectively. Simultaneously, for Sub-5, the SRCBO-MHSR model achieved a higher accuracy of 94.04%, while the CW-CNN, SCSSP, DFFN, and EEG-DMV models provided a lower accuracy of 64.11%, 51.78%, 62.72%, and 65.78%, respectively.

To demonstrate the improved performance analysis of the SRCBO-MHSR technique, a comparison study was conducted with respect to kappa. The experimental results show that the SRCBO-MHSR algorithm achieved better performance than the other methods with maximum kappa values for all subjects. For example, for Sub-1, the SRCBO-MHSR technique has achieved a superior kappa of 92.27%, while the CW-CNN, SCSSP, DFFN, and EEG-DMV techniques have achieved lower kappa of 83.15%, 75.13%,

71.26%, and 83.98%, respectively. At the same time, for Sub-5, the SRCBO-MHSR method achieved a maximum kappa of 93.31%, while the CW-CNN, SCSSP, DFFN, and EEG-DMV models had a reduced kappa of 52%, 30.15%, 33.08%, and 51.67%, respectively.

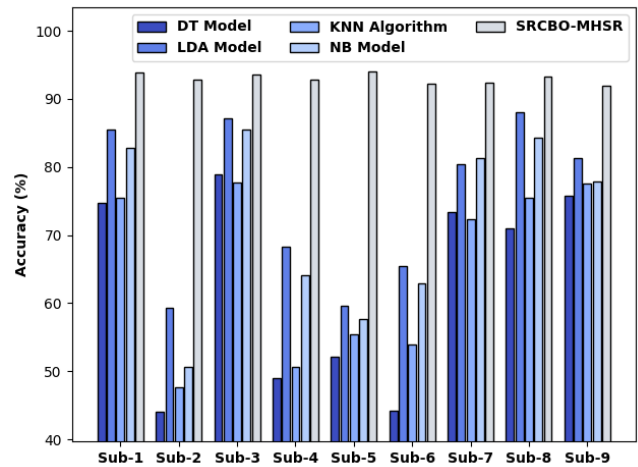


Fig. 8. Comparative analysis of the SRCBO-MHSR technique with Traditional Method Accuracy

Fig. 8 shows an improved performance analysis of the SRCBO-MHSR technique, with comparison study [23] in terms of accuracy. The experimental results show that the SRCBO-MHSR methodology achieved optimal performance over the other methods with maximum accuracy values in all subjects. For example, for Sub-1, the SRCBO-MHSR model has achieved a maximum accuracy of 93.88%, while the Decision Tree (DT), Linear Discriminant Analysis (LDA), K-Nearest Neighbor (KNN), and Naïve Bayes (NB) techniques have achieved minimum accuracy of 74.66%, 85.48%, 75.48%, and 82.75%, respectively. At the same time, for Sub-5, the SRCBO-MHSR algorithm has achieved a higher accuracy of 94.04%, while the DT, LDA, KNN, and NB techniques had lower accuracy of 52.15%, 59.67%, 55.38%, and 57.61%, respectively.

From the above results and discussion, it can be seen that the SRCBO-MHSR model is an effective tool for classifying EEG motor imagery.

CONCLUSION

In this article, a new ODLR-EEGSM technique approach for EEG motor imagery classification for BCI systems was developed. The presented ODLR-EEGSM technique approach includes VMD-based pre-processing, SSAE-based feature extraction, DWNN-based classifier, and CDFA-based parameter optimization. The application of CDFA for parameter tuning of the DWNN model (i.e., tuning the weight and bias values of the DWNN model) helps to improve the classification results. Experimental evaluation of the ODLR-EEGSM technique is performed on a benchmark dataset and the results are evaluated from various aspects. Extensive comparative results indicated the promising performance of the ODLR-EEGSM technique over the recent approaches. In the future, the classification performance of the ODLR-EEGSM technique can be boosted by the hybrid DL based feature extractors.

DATA AVAILABILITY STATEMENT

Available on Request. The datasets generated and/or analyzed during the current study are not publicly available due to the extent of the submitted research. They are available upon reasonable request from the corresponding author.

REFERENCES

- [1] Stephe, S., Jayasankar, T., Vinoth Kumar, K. (2022). Motor imagery EEG recognition using deep generative adversarial network with EMD for BCI applications. *Technical Gazette*, 29 (1), 92-100. <https://doi.org/10.17559/TV-20210121112228>
- [2] León, J., Escobar, J. J., Ortiz, A., Ortega, J., González, J., Martín-Smith, P., Gan, J. Q., Damas, M. (2020). Deep learning for EEG-based Motor Imagery classification: Accuracy-cost trade-off. *PLOS One*, 15 (6), e0234178. <https://doi.org/10.1371/journal.pone.0234178>
- [3] Khan, J., Bhatti, M. H., Khan, U. G., Iqbal, R. (2019). Multiclass EEG motor-imagery classification with sub-band common spatial patterns. *EURASIP Journal on Wireless Communications and Networking*, 174. <https://doi.org/10.1186/s13638-019-1497-y>
- [4] Lee, H. K., Choi, Y.-S. (2018). A convolution neural networks scheme for classification of motor imagery EEG based on wavelet time-frequency image. In *2018 International Conference on Information Networking (ICOIN)*. IEEE, 906-909. <https://doi.org/10.1109/ICOIN.2018.8343254>
- [5] Amin, S. U., Altaheri, H., Muhammad, G., Alsulaiman, M., Abdul, W. (2021). Attention based Inception model for robust EEG motor imagery classification. In *2021 IEEE International Instrumentation and Measurement Technology Conference (I2MTC)*. IEEE. <https://doi.org/10.1109/I2MTC50364.2021.9460090>
- [6] Al-Saegh, A., Dawwd, S. A., Abdul-Jabbar, J. M. (2021). Deep learning for motor imagery EEG-based classification: A review. *Biomedical Signal Processing and Control*, 63, 102172. <http://dx.doi.org/10.1016/j.bspc.2020.102172>
- [7] Altaheri, H., Muhammad, G., Alsulaiman, M., Amin, S. U., Altuwaijri, G. A., Abdul, W., Bencherif, M. A., Faisal, M. (2023). Deep learning techniques for classification of electroencephalogram (EEG) motor imagery (MI) signals: A review. *Neural Computing and Applications*, 35, 14681-14722. <https://doi.org/10.1007/s00521-021-06352-5>
- [8] Bang, J.-S., Lee, M.-H., Fazli, S., Guan, C., Lee, S.-W. (2022). Spatio-spectral feature representation for motor imagery classification using convolutional neural networks. *IEEE Transactions on Neural Networks and Learning Systems*, 33 (7), 3038-3049. <https://doi.org/10.1109/tnnls.2020.3048385>
- [9] Bria, A., Marrocco, C., Tortorella, F. (2021). Sinc-based convolutional neural networks for EEG-BCI-based motor imagery classification. In *Pattern Recognition: ICPR International Workshops and Challenges*. Springer, LNCS 12661, 526-535. https://doi.org/10.1007/978-3-030-68763-2_40
- [10] Yang, L., Song, Y., Ma, K., Xie, L. (2021). Motor imagery EEG decoding method based on a discriminative feature learning strategy. *IEEE Transactions on Neural Systems and Rehabilitation Engineering*, 29, 368-379. <https://doi.org/10.1109/tnsre.2021.3051958>
- [11] Altuwaijri, G. A., Muhammad, G. (2022). A multibranch of convolutional neural network models for electroencephalogram-based motor imagery classification. *Biosensors*, 12 (1), 22. <https://doi.org/10.3390%2Fbios12010022>
- [12] Huang, W., Chang, W., Yan, G., Yang, Z., Luo, H., Pei, H. (2022). EEG-based motor imagery classification using convolutional neural networks with local reparameterization trick. *Expert Systems with Applications*, 187, 115968. <http://dx.doi.org/10.1016/j.eswa.2021.115968>
- [13] Mirzaei, S., Ghasemi, P. (2021). EEG motor imagery classification using dynamic connectivity patterns and convolutional autoencoder. *Biomedical Signal Processing and Control*, 68, 102584. <https://doi.org/10.1016/j.bspc.2021.102584>
- [14] Musallam, Y. K., AlFassam, N. I., Muhammad, G., Amin, S. U., Alsulaiman, M., Abdul, W., Altaheri, H., Bencherif, M. A., Algabri, M. (2021). Electroencephalography-based motor imagery classification using temporal convolutional network fusion. *Biomedical Signal Processing and Control*, 69, 102826. <https://doi.org/10.1016/j.bspc.2021.102826>
- [15] Zhang, C., Kim, Y.-K., Eskandarian, A. (2021). EEG-inception: An accurate and robust end-to-end neural network for EEG-based motor imagery classification. *Journal of Neural Engineering*, 18 (4), 046014. <https://doi.org/10.1088/1741-2552/abed81>
- [16] Majoros, T., Oniga, S. (2021). Comparison of motor imagery EEG classification using feedforward and convolutional neural network. In *IEEE EUROCON 2021 - 19th International Conference on Smart Technologies*. IEEE, 25-29. <https://doi.org/10.1109/EUROCON52738.2021.9535592>

Received August 02, 2023
Accepted October 25, 2023